



This is a repository copy of *Finite Difference and Finite Element Simulation of a Flexible Manipulator*.

White Rose Research Online URL for this paper:
<http://eprints.whiterose.ac.uk/80507/>

Monograph:

Tokhi, M.O., Mohammed, Z. and Azad, A.K.M. (1996) Finite Difference and Finite Element Simulation of a Flexible Manipulator. Research Report. ACSE Research Report 617 .
Department of Automatic Control and Systems Engineering

Reuse

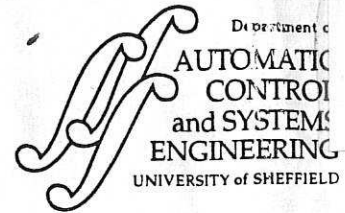
Unless indicated otherwise, fulltext items are protected by copyright with all rights reserved. The copyright exception in section 29 of the Copyright, Designs and Patents Act 1988 allows the making of a single copy solely for the purpose of non-commercial research or private study within the limits of fair dealing. The publisher or other rights-holder may allow further reproduction and re-use of this version - refer to the White Rose Research Online record for this item. Where records identify the publisher as the copyright holder, users can verify any specific terms of use on the publisher's website.

Takedown

If you consider content in White Rose Research Online to be in breach of UK law, please notify us by emailing eprints@whiterose.ac.uk including the URL of the record and the reason for the withdrawal request.



eprints@whiterose.ac.uk
<https://eprints.whiterose.ac.uk/>



629
.8
(S)

FINITE DIFFERENCE AND FINITE ELEMENT SIMULATION OF A FLEXIBLE MANIPULATOR

M O Tokhi^{*}, Z Mohamed^{**} and A K M Azad^{*}

^{*} Department of Automatic Control and Systems Engineering,
The University of Sheffield, Mappin Street, Sheffield, S1 3JD, UK.

Tel: + 44 (0)114 282 5136.
Fax: + 44 (0)114 273 1729.
E-mail: O.Tokhi@sheffield.ac.uk.

^{**} Department of Electronic Engineering,
University of Technology Malaysia, Malaysia.

Research Report No. 617

February 1996

200328366



Abstract

This paper presents a comparative investigation into the dynamic characterisation of flexible manipulators on the basis of accuracy, computational efficiency and computational requirements using finite difference (FD) and finite element (FE) methods. A constrained planar single-link flexible manipulator is considered. finite-dimensional simulations of the manipulator are developed using FD and FE methods. The simulation algorithms thus developed are implemented on two computing domains and their performances on the basis of accuracy in characterising the behaviour of the manipulator and computational efficiency are assessed.

Key words: Discrete simulation, finite difference method, finite element method, flexible manipulators.

CONTENTS

Title	i
Abstract	ii
Contents	iii
List of tables and figures	iv
1 Introduction	1
2 The flexible manipulator system	2
3 Simulation algorithms	4
3.1 Finite difference algorithm	4
3.2 Finite element algorithm	6
4 Implementations and results	9
4.1 Finite difference simulation	10
4.2 Finite element simulation	14
4.3 Comparative performance of the algorithms	16
5 Conclusion	18
6 References	20

LIST OF TABLES AND FIGURES

- Table 1: Modes of vibration of the system with number of FD sections.
- Table 2: Execution times of the computing domains with number of FD sections.
- Table 3: Modes of vibration of the system with number of FE elements.
- Table 4: Execution times of the computing domains with number of FE elements.
-
- Figure 1: Description of the flexible manipulator system.
- Figure 2: Input torque applied at the hub of the manipulator.
- Figure 3: FD simulated response of the system at the end-point using 20 sections;
(a) Time-domain. (b) Spectral density.
- Figure 4: Execution times of the computing domains with number of FD sections.
- Figure 5: Speedup with SPARC relative to 486DX in implementing the FD algorithm.
- Figure 6: FE simulated response of the system at the end-point using one element;
(a) Time-domain. (b) Spectral density.
- Figure 7: Execution times of the computing domains with number of FE elements.
- Figure 8: Speedup with SPARC relative to 486DX in implementing the FE algorithm.
- Figure 9: Execution times in implementing the algorithms characterising the system modes; (a) on the 486DX processor. (b) on the SPARC processor.
- Figure 10: Execution time speedup with the FE algorithm in comparison to the FD algorithm.

1 Introduction

Flexible manipulator systems offer several advantages over their traditional counterparts. These include light weight, faster system response, less power consumption, requiring smaller actuators, more manoeuvrable, more transportable, reduced non-linearity owing to elimination of gearing, safer operation due to reduced inertia and in general less overall cost (Azad, 1995; Meng and Chen, 1988). However, the control of flexible manipulators is made complicated by the highly non-linear dynamics of the system which involve complex processes. Therefore, flexible robots have not been much favoured, in the past, in production industries as the manipulator is required to have a reasonable end-point accuracy in response to input commands. If the advantages associated with lightweight are not to be sacrificed, efficient controls have to be studied and developed.

In order to control flexible manipulators efficiently, they must be modelled accurately. A further requirement is the efficiency in obtaining the model. An accurate model will result in a satisfactory and good control. Various approaches have previously been developed for modelling of flexible manipulators (Azad, 1995). These can be divided into two categories. The first approach looks at obtaining approximate modes by solving the partial differential equation (PDE) characterising the dynamic behaviour of a flexible manipulator system. Previous investigations at utilisation of a linear state-space model for a single-link flexible manipulator have shown that the model eigen values agree well with experimentally determined frequencies of the vibratory model (Cannon and Schmitz, 1984; Hastings and Book, 1987). The second approach uses numerical analysis methods to solve the PDE. These include the finite difference (FD) method (Tokhi and Azad, 1995) and the finite element (FE) method (Meng and Chen, 1988; Usoro et.al, 1986). In this investigation the FD and FE methods are considered. These methods allow the development of suitable simulation environments that can be utilised for real-time dynamic characterisation of the system and for test and verification of controller designs.

The FD method has previously been utilised in the dynamic characterisation of flexible beam and flexible manipulator systems (Azad, 1995; Kourmoulis, 1990; Tokhi and Azad, 1995). The method involves discretising the system into several sections (segments) and

developing a linear relation for the deflection of end of each segment using FD approximations. This method is simple in mathematical terms and is found to be more suitable for uniform structures.

The FE method has been successfully used to solve many material and structural problems (Meng and Chen, 1988; Usoro et.al, 1986). The method involves discretising the actual system into a number of elements whose elastic and inertia properties are obtained from the system. This provides approximate static and dynamic properties of the actual system. the FE method is found to be more suitable for structures of irregular nature with mixed boundary conditions.

The aim of this work is to investigate the performance of the FD and FE methods in the simulation of flexible manipulators on the basis of accuracy, computational efficiency and computational requirements. Not much work has been done on such a comparative study of the FD and FE methods in the dynamic characterisation of flexible manipulator systems. A constrained planar single-link flexible manipulator is considered. A finite-dimensional simulation of the manipulator is developed using FD and FE methods. The simulation algorithms are implemented on two computing domains and their performances, on the basis of accuracy and computational efficiency, are assessed.

2 The flexible manipulator systems

The single-link flexible manipulator considered in this paper is described in Figure 1, where, I_h represents the hub inertia of the manipulator. A payload mass M_p with its associated inertia I_p is attached to the end-point. A control torque $\tau(t)$ is applied at the hub by an actuator motor. The angular displacement of the manipulator, in moving in the POQ - plane, is denoted by $\theta(t)$. The manipulator is assumed to be stiff in vertical bending and torsion, thus, allowing it to vibrate (be flexible) dominantly in the horizontal direction. The shear deformation and rotary inertia effects are also ignored.

For an angular displacement θ and an elastic deflection u the total (net) displacement $y(x, t)$ of a point along the manipulator at a distance x from the hub can be described as a

function of both the rigid body motion $\theta(t)$ and elastic deflection $u(x, t)$ measured from the line OX ;

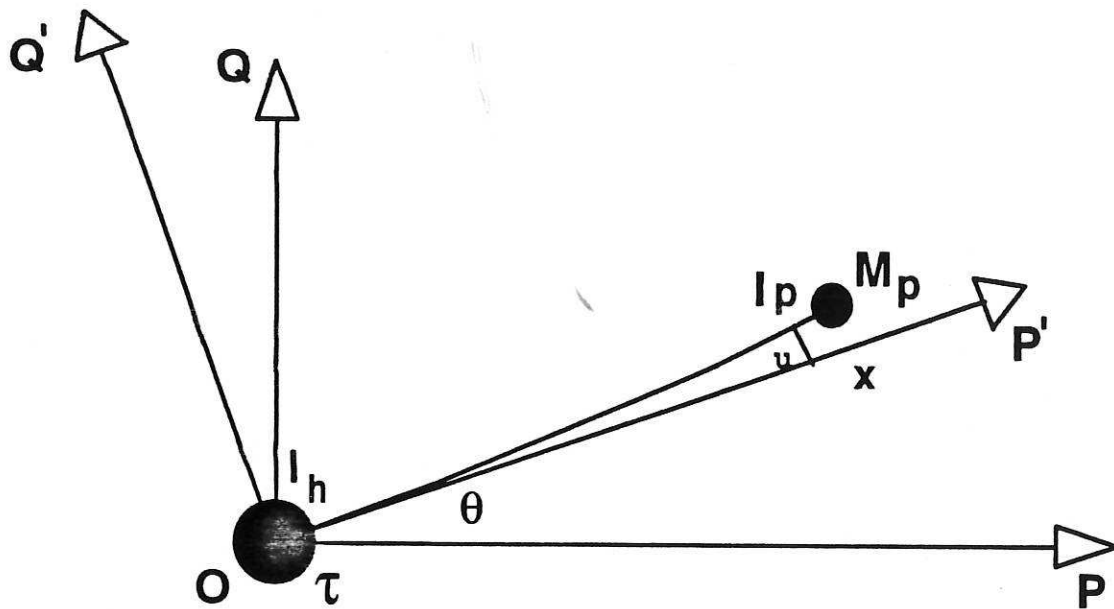


Figure 1: Description of the flexible manipulator system.

$$y(x, t) = x\theta(t) + u(x, t) \quad (1)$$

The dynamic equations of motion of the manipulator can be obtained using the Hamilton's extended principle (Meirovitch, 1967) with the associated kinetic, potential and dissipated energies of the system. The governing equation of motion of the manipulator can thus be obtained as (Tokhi and Azad, 1996)

$$EI \frac{\partial^4 y(x, t)}{\partial x^4} + \rho \frac{\partial^2 y(x, t)}{\partial t^2} = \tau(t) \quad (2)$$

with the corresponding boundary and initial conditions as

$$y(0, t) = 0, \quad I_h \frac{\partial^3 y(0, t)}{\partial x \partial t^2} - EI \frac{\partial^2 y(0, t)}{\partial x^2} = \tau(t)$$

$$M_p \frac{\partial^2 y(L, t)}{\partial t^2} - EI \frac{\partial^3 y(L, t)}{\partial x^3} = 0, \quad EI \frac{\partial^2 y(L, t)}{\partial x^2} = 0$$

$$y(x, 0) = 0, \quad \frac{\partial y(x, 0)}{\partial x} = 0$$

where E , ρ , I and L represent the Young modulus, mass density, area moment of inertia and length of the manipulator respectively. Equation (2) gives the fourth-order PDE which represents the dynamic equation describing the motion of the flexible manipulator with no structural damping.

3 Simulation algorithms

In this section the FD and FE based simulation algorithms of the manipulator are developed.

3.1 Finite difference algorithm

The PDE in equation (2) describing the dynamics of the flexible manipulator system is of a hyperbolic type and can be classified as a boundary value problem. This can be solved using an FD method. This involves dividing the manipulator length and movement time each into suitable number of sections of equal length represented by Δx ($x = i\Delta x$) and Δt ($t = j\Delta t$), where i and j are non-negative integer numbers, respectively. For end of each section (grid-point) a Taylor series expansion is used to generate the central difference formulae for the partial derivative terms of the response $y(x, t)$ of the manipulator at points $x = i\Delta x$, $t = j\Delta t$ (Burden and Faires, 1989; Lapidus, 1982). This gives

$$\begin{aligned}
 \frac{\partial^2 y(x, t)}{\partial t^2} &= \frac{y_{i, j+1} - 2y_{i, j} + y_{i, j-1}}{\Delta t^2} \\
 \frac{\partial^2 y(x, t)}{\partial x^2} &= \frac{y_{i+1, j} - 2y_{i, j} + y_{i-1, j}}{\Delta x^2} \\
 \frac{\partial^4 y(x, t)}{\partial x^4} &= \frac{y_{i+2, j} - 4y_{i+1, j} + 6y_{i, j} - 4y_{i-1, j} + y_{i-2, j}}{\Delta x^4} \\
 \frac{\partial^3 y(x, t)}{\partial x^3} &= \frac{y_{i+2, j} - 2y_{i+1, j} - 2y_{i-1, j} + y_{i-2, j}}{2\Delta x^3} \\
 \frac{\partial^3 y(x, t)}{\partial t^2 \partial x} &= \frac{y_{n-1, j+1} - 2y_{n-1, j} + y_{n-1, j-1} - y_{n, j+1} + 2y_{n, j} - y_{n, j-1}}{2\Delta x \Delta t^2}
 \end{aligned} \tag{3}$$

where, $y_{i, j}$ represents the response $y(x, t)$ at $x = i\Delta x$ and $t = j\Delta t$. Note that, a time-space discretisation is adopted in the evaluation of the response of the manipulator.

To solve the PDE in equation (2), a set of equivalent difference equations defined by the central FD quotients to replace the PDE are obtained. The manipulator is divided into a suitable number of sections of equal lengths and a difference equation, corresponding to each point of the grid is developed. The known boundary conditions are utilised to eliminate the displacements of the fictitious points outside the defined interval.

Substituting for $\frac{\partial^2 y}{\partial t^2}$ and $\frac{\partial^4 y}{\partial x^4}$ from equation (3) into equation (2) and simplifying

yields

$$y_{i,j+1} = -c[y_{i-2,j} + y_{i+2,j}] + b[y_{i-1,j} + y_{i+1,j}] + ay_{i,j} - y_{i,j-1} + \frac{\Delta t^2}{\rho} \tau(i, j) \quad (4)$$

where, $c = \Delta t^2 EI / \rho \Delta x^4$, $a = 2 - 6c$ and $b = 4c$.

Equation (4) gives the displacement of section i of the manipulator at time step $j + 1$.

Using matrix notation, this can be written as

$$\mathbf{Y}_{i,j+1} = \mathbf{A}\mathbf{Y}_{i,j} - \mathbf{Y}_{i,j-1} + \mathbf{B}\mathbf{F} \quad (5)$$

where,

$$\mathbf{Y}_{i,j+1} = \begin{bmatrix} y_{1,j+1} \\ y_{2,j+1} \\ \vdots \\ y_{n,j+1} \end{bmatrix}, \quad \mathbf{Y}_{i,j} = \begin{bmatrix} y_{1,j} \\ y_{2,j} \\ \vdots \\ y_{n,j} \end{bmatrix}, \quad \mathbf{Y}_{i,j-1} = \begin{bmatrix} y_{1,j-1} \\ y_{2,j-1} \\ \vdots \\ y_{n,j-1} \end{bmatrix}$$

$$\mathbf{A} = \begin{bmatrix} m_1 & m_2 & m_3 & 0 & 0 & \cdots & 0 & 0 & 0 & 0 & 0 \\ b & a & -b & -c & 0 & \cdots & 0 & 0 & 0 & 0 & 0 \\ -c & b & a & b & -c & \cdots & 0 & 0 & 0 & 0 & 0 \\ \ddots & \ddots \\ 0 & 0 & 0 & 0 & 0 & \cdots & -c & b & a & b & -c \\ 0 & 0 & 0 & 0 & 0 & \cdots & 0 & m_{11} & m_{12} & m_{13} & m_{14} \\ 0 & 0 & 0 & 0 & 0 & \cdots & 0 & m_{21} & m_{22} & m_{23} & m_{24} \end{bmatrix}$$

$$\mathbf{F} = \begin{bmatrix} \tau(i, j) \\ 0 \\ \vdots \\ 0 \end{bmatrix}, \quad \mathbf{B} = \frac{\Delta t^2}{\rho}$$

The values of m_1 to m_3 and m_{11} to m_{24} in matrix \mathbf{A} are determined from the boundary and initial conditions related to the dynamic equation of the flexible manipulator system

(Tokhi and Azad, 1995). Equation (5) is the general solution of the PDE, giving the displacement of section i of the manipulator at time step $j+1$, which can easily be implemented on a digital processor.

It follows from equation (5) that, to obtain the displacements $y_{i,j+1}$, $y_{n-1,j+1}$ and $y_{n,j+1}$ the displacements of the fictitious points $y_{-1,j}$, $y_{n+1,j}$ and $y_{n+2,j}$ are required. These are obtained using the boundary and initial conditions related to the dynamic equation of the flexible manipulator system (Tokhi and Azad, 1995). The stability of the algorithm can be examined by ensuring that the iterative scheme described in equation (5) converges to a solution. The necessary and sufficient condition for stability satisfying this convergence requirement is given by $0 \leq c \leq 0.25$ (Kourmoulis, 1990; Tokhi and Azad, 1995).

3.2 Finite element algorithm

Since its introduction in the 1950s, the FE method has been continually developed and improved (Fagan, 1992; Rao, 1989). The FE method involves decomposing the mechanical structure into several simple pieces or elements. The elements are assumed to be interconnected at certain points known as nodes. For each element, an equation describing the behaviour of the element is obtained through an approximation technique. The elemental equations are then assembled together to form the system equation. It is found that by reducing the element size of the structure, that is, increasing the number of elements, the overall solution of the system equation can be made to converge to the exact solution.

The main steps in an FE analysis include (1) discretisation of the structure into elements, (2) selection of an approximating function to interpolate the result, (3) derivation of the basic element equation, (4) calculation of the system equation, (5) incorporation of the boundary conditions and (6) solving the system equation with the inclusion of the boundary conditions. In this manner, the flexible manipulator is treated as an assemblage of n elements and the development of the algorithm can be divided into three main parts: the

FE analysis, state-space representation and obtaining the system outputs. A brief outline of this process is given below.

Using the FE method to solve dynamic problems leads to the well-known equation (Rao, 1989)

$$u(x, t) = N(x)Q(t) \quad (6)$$

where $Q(t)$ and $N(x)$ represent the nodal displacement and shape function respectively. For the flexible manipulator under consideration, $u(x, t)$ in equation (6) represents the residual motion.

Substituting for $u(x, t)$ from equation (6) into equation (1) and simplifying yields

$$y(x, t) = N(x)^* Q(t)^* \quad (7)$$

where

$$Q(t)^* = [\theta(t) \quad Q(t)]^T, \quad N(x)^* = [x \quad N(x)]$$

Using the above, the element mass matrix M^e and stiffness matrix K^e can be obtained as (Mohamed, 1995)

$$M^e = \rho A \int_0^L (N^*)^T (N^*) dx$$

$$K^e = EI \int_0^L (B^*)^T B^* dx$$

where A and L are the cross-sectional area and length of the manipulator respectively and $B^* = d^2 N^* / dx^2$.

The new shape function N^* and nodal displacement vector Q^* in equation (7) incorporate local and global variables. Among these, the angle $\theta(t)$ and the distance x are global variables while $N(x)$ and $Q(t)$ are local variables when the link is divided into n elements. Defining $s = x - \sum_{i=1}^{n-1} l_i$, where l_i is the length of the i th element, as a local variable of the n th element, the new element mass matrix and stiffness matrix can be obtained for the n elements as (Mohamed, 1995)

$$M^n = \frac{\rho Al}{420} \begin{bmatrix} m(1,1) & m(1,2) & m(1,3) & m(1,4) & m(1,5) \\ m(1,2) & 156 & 22l & 54 & -13l \\ m(1,3) & 22l & 4l^2 & 13l & -3l^2 \\ m(1,4) & 54 & 13l & 156 & -22l \\ m(1,5) & -13l & -3l^2 & -22l & 4l^2 \end{bmatrix}$$

$$K^n = \frac{EI}{l^3} \begin{bmatrix} 0 & 0 & 0 & 0 & 0 \\ 0 & 12 & 6l & -12 & 6l \\ 0 & 6l & 4l^2 & -6l & 2l^2 \\ 0 & -12 & -6l & 12 & -6l \\ 0 & 6l & 2l^2 & -6l & 4l^2 \end{bmatrix}$$

where l is the elemental length and

$$m(1,1) = 140(\rho Al^2)(3n^2 - 3n + 1)$$

$$m(1,2) = m(2,1) = 21(\rho Al)(10n - 7)$$

$$m(1,3) = m(3,1) = 7(\rho Al^2)(5n - 3)$$

$$m(1,4) = m(4,1) = 21(\rho Al)(10n - 3)$$

$$m(1,5) = m(5,1) = -7(\rho Al^2)(5n - 2)$$

Note in the above that, the element mass matrix depends on the element number, whereas the element stiffness matrix has the same value regardless of the element number. The element mass and stiffness matrices from above are assembled to obtain system mass and stiffness matrices, M and K , and used in the Lagrange equation to obtain the dynamic equation of the flexible manipulator as

$$M\ddot{Q}(t) + KQ(t) = F(t) \quad (8)$$

where $F(t)$ is the vector of applied forces and torques and

$$Q(t) = [\theta \quad U_1 \quad \theta_1 \quad \dots \quad U_{n+1} \quad \theta_{n+1}]^T$$

The M and K matrices in equation (8) are of size $m \times m$ and $F(t)$ is of size $m \times 1$, $m = 2n + 1$. For the manipulator, considered as a pinned-free arm, with the applied torque τ at the hub, the flexural and rotational displacement, velocity and acceleration at the hub are zero at $t = 0$ and the external force is $F(t) = [\tau \quad 0 \quad \dots \quad 0]^T$. Moreover, in this work it is assumed that $Q(0) = 0$.

The matrix differential equation in equation (8) can be represented in a state-space form as

$$\begin{aligned}\dot{v} &= Av + Bu \\ y &= Cv + Du\end{aligned}$$

where

$$\begin{aligned}A &= \left[\begin{array}{c|c} 0_m & I_m \\ \hline -M^{-1}K & 0_m \end{array} \right], & B &= \begin{bmatrix} 0_{m \times 1} \\ M^{-1} \end{bmatrix} \\ C &= [0_m \quad I_m], & D &= [0_{2m \times 1}]\end{aligned}$$

0_m is an $m \times m$ null matrix, I_m is an $m \times m$ identity matrix, $0_{m \times 1}$ is an $m \times 1$ null vector,

$$u = [\tau \quad 0 \quad \dots \quad 0]^T.$$

$$v = \begin{bmatrix} \theta & U_2 & \theta_2 & \dots & U_{n+1} & \theta_{n+1} \\ \dot{\theta} & \dot{U}_2 & \dot{\theta}_2 & \dots & \dot{U}_{n+1} & \dot{\theta}_{n+1} \end{bmatrix}^T$$

Solving the state-space representation gives the vector of states v , that is, the angular, nodal flexural and rotational displacements and velocities.

4 Implementations and results

To implement the FD and FE algorithms an aluminium type flexible manipulator of dimensions $960 \times 19.23 \times 3.2 \text{ mm}^3$, mass density 2710 kg/m^3 , inertia 0.0495 kgm^2 and $I = 5.1924 \times 10^{-11} \text{ m}^2$ is considered. The first three modes of vibration of the manipulator, obtained analytically, are at 12.73 Hz, 36.98 Hz and 89.65 Hz (Azad, 1995). For simplicity purposes, the effects of hub inertia and payload are ignored. The simulation algorithms thus developed are coded within MATLAB (The Math Works, 1995) and implemented on two general purpose computing domains, namely a 486DX (33 MHz) PC and a Sun 4-ELC (33 MHz) SPARC station. A bang-bang input of amplitude 0.1 Nm, shown in Figure 2, is used as input torque and the system response is obtained and analysed over a period of 1.2 sec.

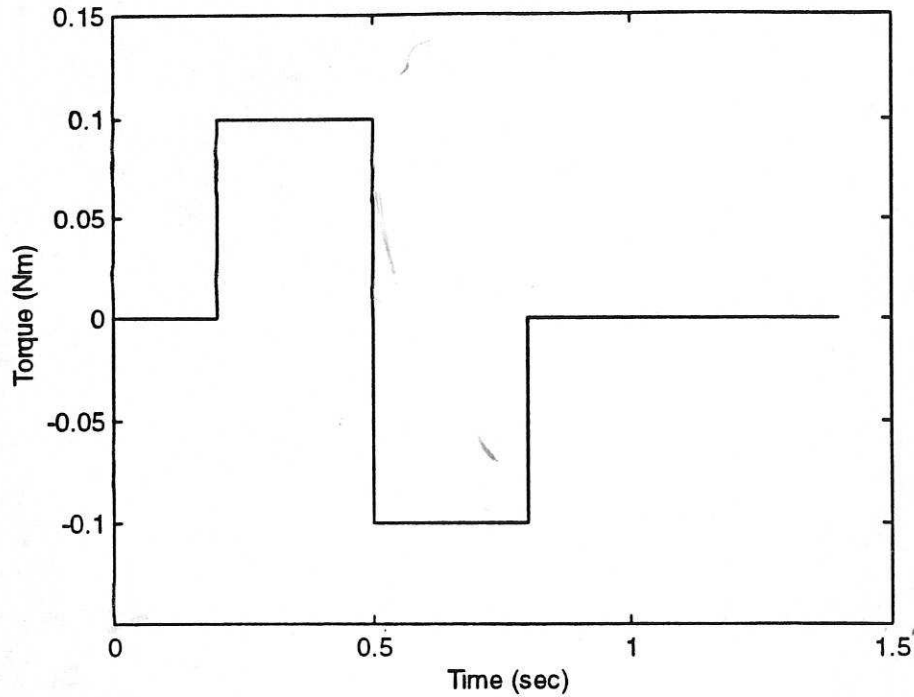
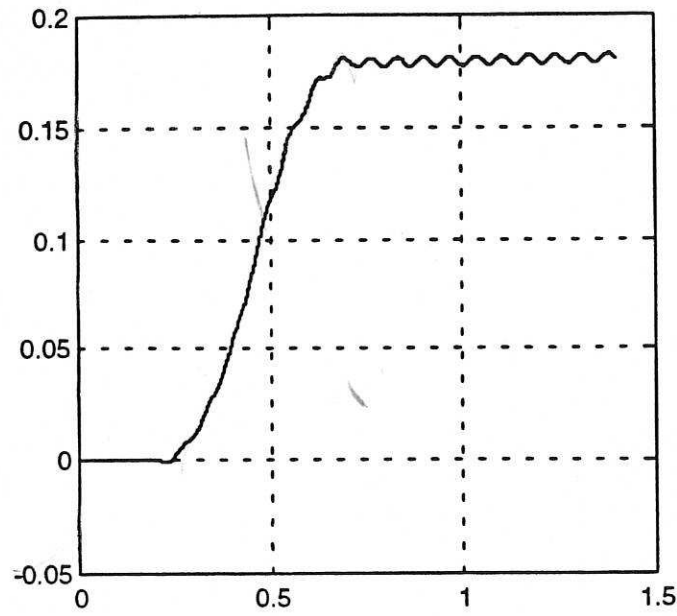


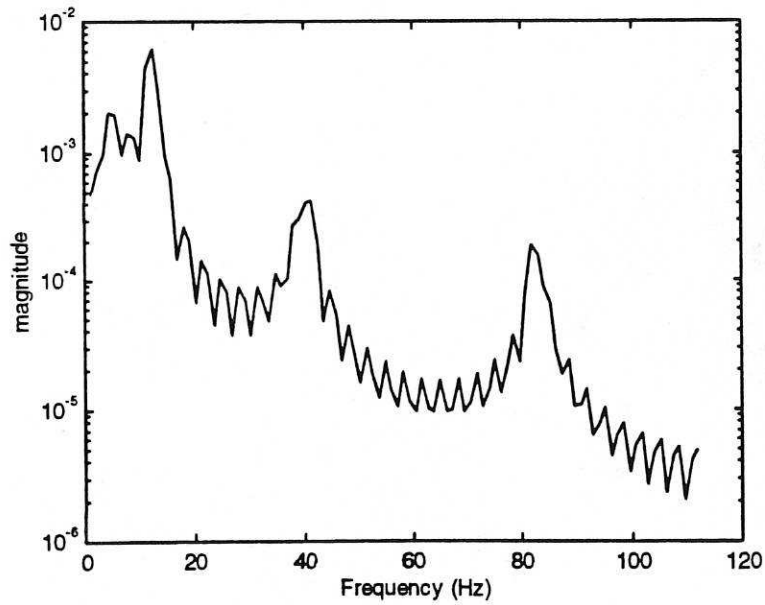
Figure 2: Input torque applied at the hub of the manipulator.

4.1 Finite difference simulation

To investigate the accuracy of the FD simulation in characterising the behaviour of the system, the algorithm was implemented on the basis of varying number of sections along the link from 5 to 20. Figure 3 shows the simulated time-domain and corresponding spectral density of the system response at the end-point using 20 sections. It is noted that the first three modes of vibration of the system occur at 12.4352 Hz, 41.3472 Hz and 81.7417 Hz respectively. These are reasonably close to the corresponding analytical values. Table 1 shows the first three resonance modes of the system and the corresponding percent errors relative to the analytical values with the algorithm using various number of sections. These were obtained, in a similar manner as Figure 3, through spectral analysis of the response of the system at the end-point. It is noted that the resonance frequency corresponding to the first mode of vibration of the system converges to a reasonably stable value with the algorithm using 10 sections or more and for the second and third modes with 15 and 20 sections or more respectively. It was noted that, although the responses of the



(a)



(b)

Figure 3: FD simulated response of the system at the end-point using 20 sections;
(a) Time-domain.
(b) Spectral density.

Number of sections	Mode 1		Mode 2		Mode 3	
	(Hz)		(Hz)		(Hz)	
	(12.73)	% Error	(36.98)	% Error	(89.65)	% Error
5	11.1917	12.084	33.5751	9.207	60.3109	32.727
10	12.4352	2.316	37.9275	2.562	77.4093	13.654
15	12.4352	2.316	39.5337	6.906	81.6062	8.972
20	12.4352	2.316	41.3472	11.81	81.7617	8.799

Number of sections	486DX (sec)	SPARC (sec)
5	1.4100	1.2600
10	6.9767	3.6400
15	29.9800	21.0433
20	60.7750	42.9000

system at the end-point using 5 and 20 sections were similar in character, with 20 sections a steady-state level was reached within 0.6 sec, whereas, with 5 sections the response did not fully reach a steady-state level over the 1.2 sec measurement period. It was also noted that a reasonable accuracy in characterising the behaviour of the flexible manipulator was achieved with at least 10 sections. These are evidenced in Table 1 with the errors in the resonance frequencies in comparison to the corresponding analytical values.

Table 2 and Figure 4 show the corresponding execution times achieved with the two processing domains in implementing the FD algorithm with various number of sections. As expected, the execution time increases with increasing number of sections. Moreover, it is noted that the two computing platforms appear to perform at a similar speed with lower number of sections. However, as the number of sections increase the SPARC processor outperforms the 486DX processor significantly. This, as demonstrated by the change of gradients in Figure 4, is mainly due to the run-time memory management and relatively

limited cache in the 486DX processor. This is further shown in Figure 5 by the speedup achieved with the SPARC processor in comparison to the 486DX in implementing the algorithm with various sections.

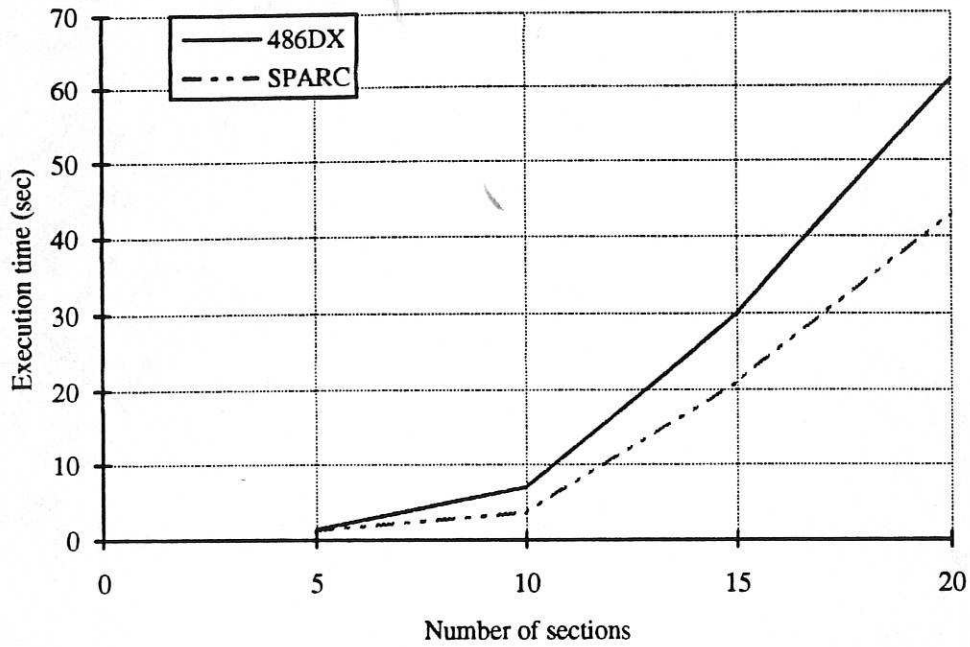


Figure 4: Execution times of the computing domains with number of FD sections.

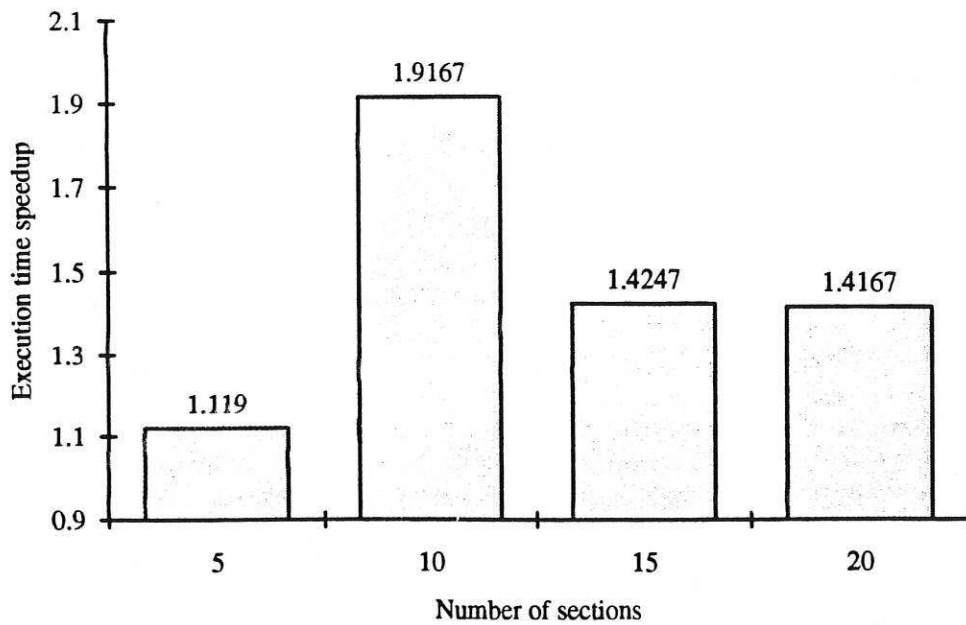


Figure 5: Speedup with SPARC relative to 486DX in implementing the FD algorithm.

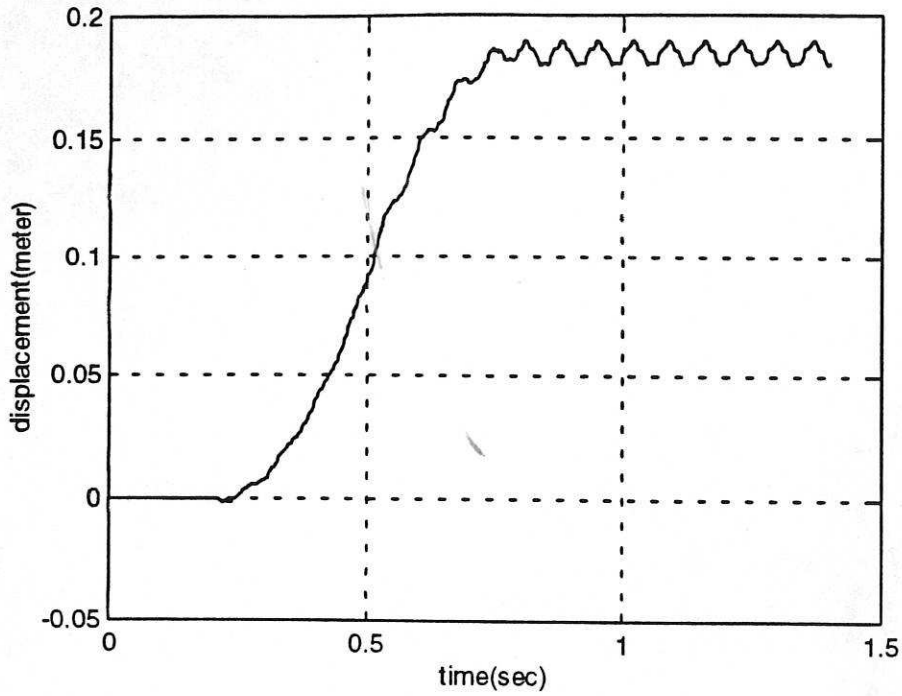
4.2 Finite element simulation

To investigate the accuracy of the FE simulation in characterising the behaviour of the system, the algorithm was implemented on the basis of varying number of elements from 1 to 20. It was noted that the response of the system at the end-point due to the bang-bang torque input reached a steady-state level within 0.6 sec with the algorithm using one or more elements. Moreover, the residual motion was found to be predominantly characterised by the first mode of vibration with one element, whereas, with more elements higher modes of vibration were also apparent. This is evidenced in Figure 6 which shows the time-domain and corresponding spectral density of the response of the system at the end-point using one element and in Table 3 which shows the resonance modes of the system in relation to the number of elements used. Although, the error in the resonance frequency of the second mode in comparison to the corresponding analytical value is relatively large with one element, this has not affected the general character of the system response as the first mode is the dominant one.

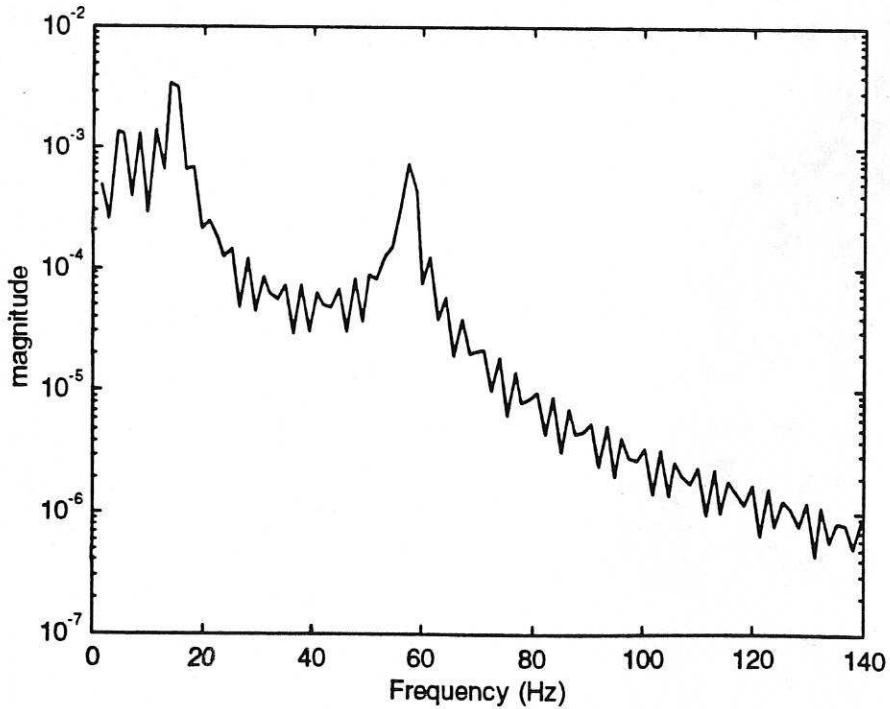
Table 3: Modes of vibration of the system with number of FE elements.

Number of elements	Mode 1 (Hz)		Mode 2 (Hz)		Mode 3 (Hz)		Mode 4 (Hz)
	(12.73)	% Error	(36.98)	% Error	(89.65)	% Error	-
1	14.509	13.975	57.306	54.965	-	-	-
2	11.9689	5.979	44.974	21.617	109.896	22.583	-
3	11.969	5.978	40.622	9.849	93.575	4.378	-
5	11.969	5.978	40.259	8.867	86.684	3.308	112.798
10	11.969	5.978	40.259	8.867	85.596	4.522	132.383
15	11.969	5.978	40.259	8.867	85.321	4.829	135.448
20	11.969	5.978	40.259	8.867	85.232	4.928	135.285

It is noted in Table 3 that the number of resonance modes identified increases with increasing number of elements. Moreover, the resonance frequency corresponding to the first mode of vibration of the system converges to a reasonably steady value with the



(a)



(b)

Figure 6: FE simulated response of the system at the end-point using one element;
(a) Time-domain.
(b) Spectral density.

algorithm using two elements or more, for the second mode with three elements or more, for the third mode with five elements or more and for the fourth mode with 10 elements or more. The corresponding execution times achieved with the two processing domains in implementing the FE algorithm with various number of elements is shown in Table 4 and Figure 7. As expected, the execution time increases with increasing number of sections. Moreover, it is noted that the SPARC processor outperforms the 486DX processor significantly. This, as demonstrated by the change of gradients in Figure 7, is mainly due to the run-time memory management and relatively limited cache in the 486DX processor. This is further shown in Figure 8 by the speedup achieved with the SPARC processor in comparison to the 486DX in implementing the algorithm with various number of elements.

Number of elements	486DX (sec)	SPARC (sec)
1	1.9067	0.8278
2	2.1933	0.9389
3	2.2733	1.0833
5	3.6667	1.4833
10	11.7333	3.9944
15	20.3800	9.3834
20	37.9000	18.7722

4.3 Comparative performance of the algorithms

It follows from the simulated results that a reasonable general characterisation of the flexible manipulator is achieved with the FD and FE methods using at least 10 sections and one element respectively. The corresponding execution times achieved in implementing the algorithms are 6.9767 and 1.9067 sec on the 486DX and 3.64 and 0.8273 sec on the SPARC processor respectively. These give execution time speedups of 3.659 and 4.4 on the 486DX and the SPARC processors respectively in implementing the FE algorithm in

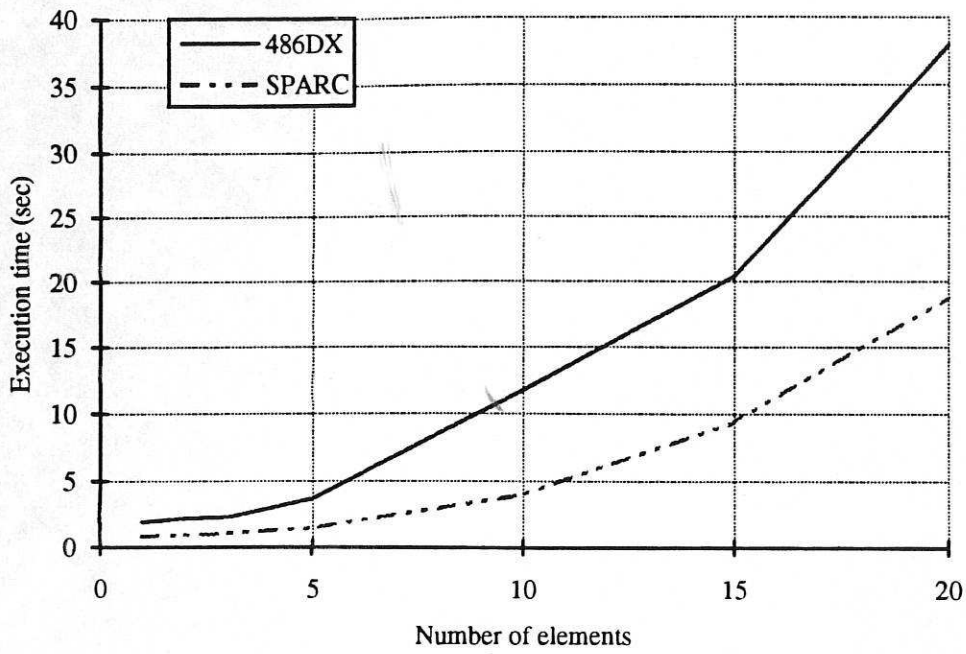


Figure 7: Execution times of the computing domains with number of FE elements.

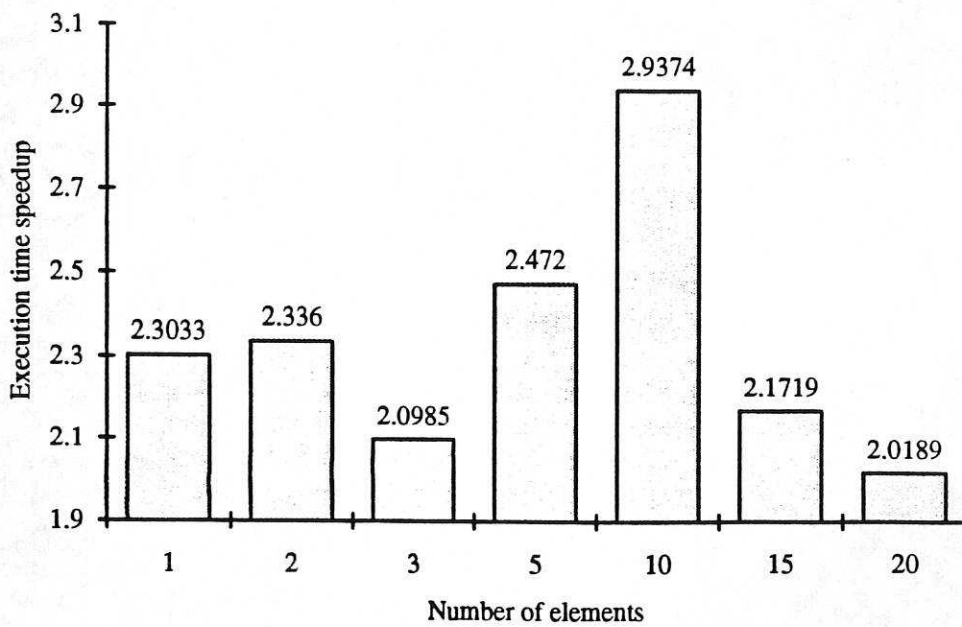
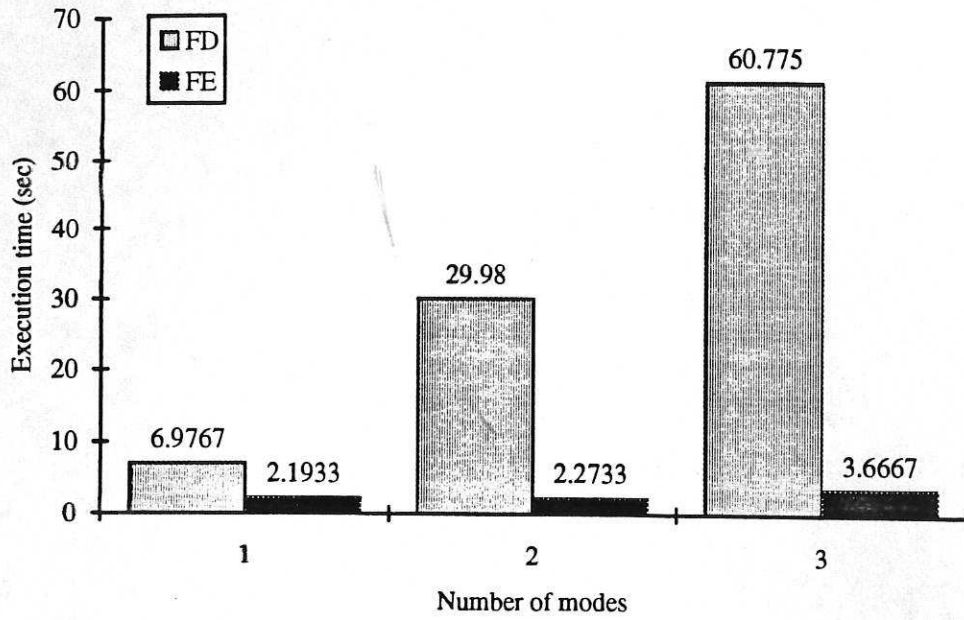


Figure 8: Speedup with SPARC relative to 486DX in implementing the FE algorithm.

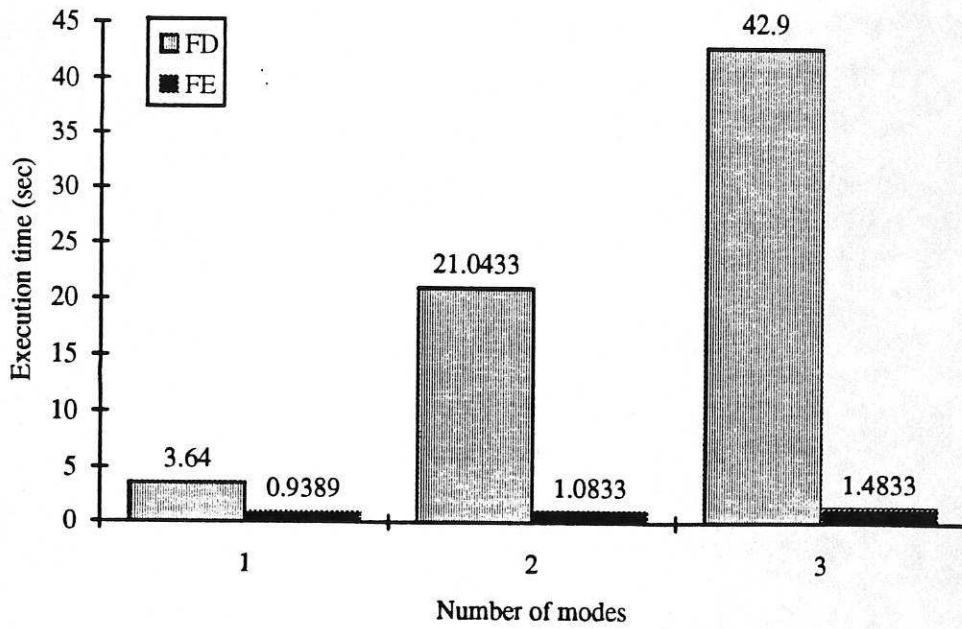
comparison to the FD algorithm. Similarly, comparing the results in Tables 1 and 3 reveals that reasonable convergence in the resonance frequency corresponding to the first resonance mode of the manipulator is achieved with the FD and FE algorithms using at least 10 sections and 2 elements respectively. With the inclusion of the second resonance mode, similar level of convergence is achieved with the FD and FE algorithms using at least 15 sections and 3 elements respectively. With the inclusion, further, of the third resonance mode, similar level of convergence is achieved with the FD and FE algorithms using at least 20 sections and 5 elements respectively. The corresponding execution times in implementing the algorithms on the 486DX and the SPARC processor achieving convergence for the first, second and third modes of vibration of the system, as extracted from Tables 2 and 4, are shown in Figure 9. The corresponding execution time speedups at achieving convergence of the resonance modes with the FE algorithm in comparison to the FD algorithm are shown in Figure 10. These results demonstrate that a more accurate and more efficient performance is achieved with the FE algorithm as compared to the FD algorithm.

5 Conclusion

A comparative performance evaluation of the FD and FE methods on the basis of accuracy and computational efficiency in the simulation of a flexible manipulator system has been presented. Simulation environments characterising the dynamic behaviour of a single-link flexible manipulator have been developed using FD and FE methods. The algorithms thus developed have been implemented on two general purpose computing domains and their performances on the basis of accuracy and computational speed have been investigated. It has been demonstrated that although the FE method is mathematically more complex than the FD method, better accuracy and efficient performance is achieved with the FE method in comparison to the FD method.



(a)



(b)

Figure 9: Execution times in implementing the algorithms characterising the system modes;
 (a) on the 486DX processor.
 (b) on the SPARC processor.

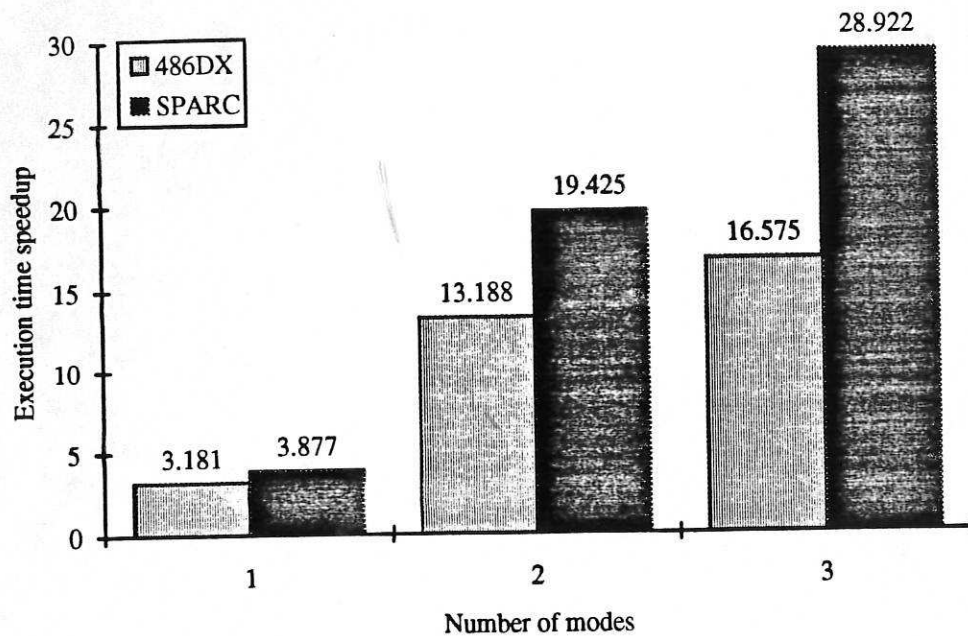


Figure 10: Execution time speedup with the FE algorithm in comparison to the FD algorithm.

6 References

- AZAD, A. K. .M. (1995). *Analysis and design of control mechanisms for flexible manipulator systems*, PhD thesis, Department of Automatic Control and Systems Engineering, The University of Sheffield, UK.
- BURDEN, R. L. and FAIRES, J. D. (1989). *Numerical analysis*, PWS-KENT Publishing Company, Boston.
- CANNON, R. H. and SCHMITZ, E. (1984). Initial experiments on the control of a flexible manipulator, *The International Journal of Robotics Research*, **3**, pp. 62-75.
- FAGAN, M. J. (1992). *Finite element analysis, theory and practice*, Longman, Harlow.
- HASTINGS, G. G. and BOOK, W. J. (1987). A linear dynamic model for flexible manipulators, *IEEE Control Systems Magazine*, **87**, (1), pp. 61-64.
- KOURMOULIS, P .K. (1990). *Parallel processing in the simulation and control of flexible beam structure systems*. PhD thesis, Department of Automatic Control and Systems Engineering, The University of Sheffield, UK.

Siti Zaiton Mohd Hashim
15 Harney Close
Darnall
Sheffield S9 5BW
UK

23 August 2001

Manager
Bank Perwira Affin Berhad
Cawangan Taman Universiti
Skudai 81310
Johor Darul Takzim

Dear Sir/Madam,

Re: Current Account Number 077 150 0000000544

I, hereby would like to inform that I am now residing in UK, doing my PhD program for 3 years or so starting from May 2001 until April 2003. I therefore would appreciate if you could send a monthly copy of my account statement to the address stated above. Please deduct any expense from my account.

Details of my current account is as below:

Branch: Taman Universiti, Skudai, Johor
Name: Siti Zaiton Mohd Hashim
A/C No.: 077 150 0000000544
S/N No.: 062551-062575

I thank you for your cooperation.

Regards,



(Siti Zaiton Mohd Hashim)

e-mail: cop00szm@shef.ac.uk